TEMPERATURE DISTRIBUTION IN A VERTICAL COOLING CRYSTALLIZER

G. D. McBAIN[1], J. A. HARRIS[2], K. F. MILLER[3], AND S. N. VIGH[4]

[1]*James Cook University, Townsville* (geordie_mcbain@yahoo.com.au)
[2]*Maunsell Australia Pty Ltd, Townsville,* [3]*Sugar Research Institute, Mackay,*
[4]*CSR Ltd, Ingham*

KEYWORDS: vertical crystallizer, temperature traverse, stirring, mixing, computational fluid dynamics, validation

Abstract

Horizontal temperature traverses were taken in Victoria Mill's vertical cooling crystallizer to test new and previously published computational fluid dynamics models. In addition to runs carried out under normal operating conditions, an experiment was performed to assess the effect of ceasing the stirring. The resulting temperature profiles presented in this paper confirm many, but not all, of the CFD predictions. The contradictions prompted a reappraisal of the role of stirring, in particular. Based on CFD, factory measurements, and analysis, a comprehensive picture of the mechanisms controlling the temperature distribution in a vertical crystallizer is derived and presented.

Introduction

Vertical continuous cooling crystallizers possess obvious advantages but persistent deviations from ideal plug-flow behaviour in vessels installed in Australia have caused operational problems and delayed the introduction of more units.

Keast and Sichter (1984) analysed cooling water energy balances and tracer residence times in an early vertical crystallizer and deduced short-circuiting, particularly for higher throughputs and massecuite-to-water temperature differences.

Dissatisfaction with that vessel led to its replacement by the vessel shown in Figure 1 and the start of the present project which seeks the causes of poor unit performance in internal flow and heat transfer details. The first stages employed the CFD code *FIDAP* (Harris *et al.*, 1995) and identified a basic heat transfer phenomenon in crystallizers: thermal boundary layer formation. Models of flow over tubes showed that cooling was confined to thin regions around the tubes and thin wakes downstream of them (see also Figure 1*b*). As discussed by Robinson (1995), this may be attributed to the material properties. The properties are expressed in two key dimensionless groups: the Reynolds number, $Re=\rho uD/\mu$, and the Péclet number, $Pe=\rho uDc/k$. Here ρ is density, u velocity, μ viscosity, c specific heat, k thermal conductivity, and D a length scale, such as the diameter of a cooling tube. At high Reynolds numbers (>>1) the flow will be unsteady or turbulent, which leads to good mixing, but $Re\sim10^{-4}$ is typical for a crystallizer cooling tube. A high Péclet number (>>1) means that thermal energy is more carried along with the stream than across it by conduction; $Pe\sim10^{3}$ is typical in the crystallizer. The combination of low Re and high Pe means that the streamlines are steady and smooth and that the temperature is largely constant along them; an exception occurs in the immediate vicinity of a cooled (or heated) surface where a thin boundary layer forms. This situation is not favourable for a

transversely uniform temperature field, as is the objective in a continuous flow vessel such as a vertical crystallizer.

The flow in a stirred crystallizer is unsteady and 3-D. This remains computationally infeasible but by assuming axial symmetry Sima and Harris (1997) obtained the first visualization of the overall temperature distribution. This involved modelling the tubes in Figure 1*a* as rings about the axis and replacing the moving stirrer with a steady body force. The results showed congealed massecuite around cooling surfaces and considerable short-circuiting, particularly down the wall between the inlet and outlet. This prompted the installing of the baffles shown in Figure 1 with a consequent narrowing of the residence time distribution (Sima and Harris, 1999).

Temperature traverses during the 1999 season

In spite of the success of the retrofitting of the baffles, model validation was desired because of the numerous simplifying assumptions that had to be made in order to apply CFD to such a large and complex vessel; particularly assumptions about the rheology (Leong *et al.*, 2001) and the reduction of an unsteady 3-D flow to a steady axisymmetric or plane flow. To stringently test the CFD, local measurements are better than such global measures as residence time and outlet temperature. As techniques for measuring local massecuite velocity are still at the experimental stage (Miller and Muddle, 2000), temperature traverses were the best available test. To this end, probes consisting of a standard thermistor and a traversing mechanism were designed and constructed, and four ports—an upper and a lower pair with a north and a south port at each level—were cut in the crystallizer for their insertion (Figure 1*c*).

The first temperature traverses were undertaken during the 1999 crushing season at both levels on the south side. The results are plotted in Figure 2, along with, for the lower probe, a *FIDAP* temperature profile (previously unpublished, but similar to Figure 3*a* of Sima and Harris 1999). The traverses show largely uniform horizontal temperature profiles with localized depressions around each cooling tube. These confirm the presence of thermal boundary layers, but overall the agreement is poor: the CFD predicts a much more uneven profile than found experimentally and there is no evidence for the predicted cool region encompassing the inner three tubes at the lower level.

Reassessment of crystallizer models

To try and find the cause of the discrepancies between the factory measurements and CFD predictions, new runs were made using the *Triangle* mesh generator (Shewchuk, 1996) and the *Fastflo* finite element package (CSIRO, 1997). A number of the assumptions were varied: fluid inertia, shear-thinning, temperature-thinning, the axisymmetric body force representing stirring, and buoyancy were omitted, and the axisymmetric geometry was replaced with a plane 2-D slice. Figure 1*b* shows a *Fastflo* temperature field with all these simplifications. None of these changes removed the discrepancy. The one that made the most difference was neglecting the temperature-thinning effect; in the lower profiles in Figure 2, the temperature-thinning *FIDAP* model predicts a cool region encompassing the three innermost tubes, whereas the constant-viscosity *Fastflo* model shows warmer passages between all tubes. This apparent improvement is problematic, however, as massecuite viscosity is certainly temperature-dependent. It was surmised that some other factor must be preventing widespread congelation (reduction in fluidity, due here to cooling), and that it might be the stirring.

Robinson (1995) considered the fluid motion caused by the stirrer arms via analogy with the classical problem of slow flow over a cylinder and argued that as the streamlines are symmetric fore and aft (see Figure 3*a*), the fluid merely parts as the arm approaches and rejoins after it passes. With no fluid distortion, the arm provides no mixing.

However, by inspecting the same analogy in a different way, another interpretation emerges. Instead of considering the paths of isolated particles (streamlines), consider the motion of a connected group of particles (material line); say a line initially perpendicular to and upstream of the cylinder. While, by the symmetry identified, each particle on the line must later pass through the corresponding point on the downstream mirror-image line, they do not have to do so simultaneously, so the line need not reform. In fact, fluid near the cylinder is slowed by viscous forces, so that the line does not reform but rather is distorted so that the arm does mix the fluid.

This may be illustrated qualitatively by calculating particle paths from an analytical approximation to the flow (Figure 3). The resulting streamlines are symmetric upstream and downstream, but the snapshots of a material line are far from symmetric. The line is indeed distorted, and in the same way the arm must distort the thin thermal wakes and congelation predicted by the CFD.

By breaking up the thermal wakes and re-establishing a uniform temperature field between rows, the stirring contributes to overall performance in two ways. First, less of the heat transfer area on lower rows is wasted on already cooled massecuite; a particular problem with in-line tube rows. Second, by eliminating excessively hot or cold regions which for a temperature-thinning fluid are prone to short-circuiting or congelation, respectively, the residence time distribution is narrowed.

Temperature traverses during the 2000 season

An experiment was carried out to test whether the stirring caused the error in the predictions. A pair of traverses was taken during normal operation, and then the stirrer was turned off. The next day, with the stirrer still turned off, the traverses were repeated. Apart from the stirring, other factors were kept as constant as possible, though this is difficult in an operating factory (see the inlet temperatures in Figure 4). The vessel was only about two-thirds full (as reflected in the CFD model in Figure 1*b*). Thus only the two lower ports could be used for the temperature traverses.

The temperature profiles (Figure 5) are very different on the two days, confirming the importance of stirring. The unstirred profiles agree much better with the CFD: the cold region on the inner south side (around –1000 mm, and also seen extending over the north side) is now distinctly present. (The agreement is still not good but there is little point pursuing this further as unstirred crystallizers are clearly impractical.)

An even more striking demonstration of the importance of stirring is provided by the inlet and outlet temperature records (Figure 4). The stirred readings show that the variations in the inlet conditions are almost entirely eliminated during passage through the vessel, but without stirring the outlet signal is highly correlated with the inlet signal and clearly indicates a significant amount of the flow passing through with minimal cooling in only ten minutes: orders of magnitude less than the nominal residence time.

Discussion and conclusions

The reason why the current stirrer counteracts nonuniform cooling has been elucidated by a simple mechanistic model which can also be used to explain why the stirring in Keast and Sichter's (1984) BMA unit was ineffective. If instead of the

vertical material line in Figure 3*b*, a horizontal line had been considered, the line, being close to a streamline, would flow over the arm with little distortion. The lesson for mixing is that the motion of the stirrer must be perpendicular to the isotherms for them to be disrupted. The BMA used cooling plates swept by scrapers; thus the stirring is basically parallel to the cooling elements and isothermal surfaces, and the mixing action is ineffective.

Similarly, the model explains why the steady body force used by Sima and Harris (1997) to represent stirring produced no mixing. The axisymmetric induced swirl was parallel to the axisymmetric cooling tubes, not perpendicular as required for mixing.

It has long been known that stirring in crystallizers is beneficial for crystal growth, and here its role in flow and heat transfer has been demonstrated. Future CFD work will need to take this into account. Some potentially promising results have been obtained by modelling the stirring as an enhancement to the thermal conductivity in the swept region, but the work is too *ad hoc* and preliminary to present here.

Acknowledgments

The authors appreciate the assistance of Craig Muddle (SRI) and the staff of Victoria Mill in carrying out the measurements, and acknowledge helpful discussions with Dr Ross Broadfoot (SRI), who also originally designed the experimental program, and Darrin Stephens (SRI). The source code to *LSODE* and *Triangle* is available at Netlib.

REFERENCES

CSIRO (1997) *Fastflo* Tutorial Guide. Numerical Algorithms Group, Oxford.

Harris, J.A., Robinson, J.A. and Vigh, S. (1995). Mathematical modelling of flow and heat transfer in a vertical crystallizer. Proc. Aust. Soc. Sugar Cane Technol., 17:216–221.

Hindmarsh, A.C. (1983). ODEPACK, a systematized collection of ODE solvers. In: Stepleman, R. S. (ed.). Scientific Computing, 55–64. North–Holland, Amsterdam.

Keast, W.J. and Sichter, N.J. (1984). Vertical continuous crystalliser—Victoria Mill. Proc. Aust. Soc. Sugar Cane. Technol., 6:293–299.

Leong, Y.K., McBain, G.D., Chu, S.Y. and Ong, B.C. (2001). Pseudoplastic and viscoelastic behaviour of molasses. Proc. Aust. Soc. Sugar Cane Technol., 23:341–345.

Miller, K.F. and Muddle, C.P. (2000). The measurement of massecuite circulation in batch and continuous pans. Proc. Aust. Soc. Sugar Cane Technol., 22:529–530.

Proudman, I. and Pearson, J.R.A. (1957). Expansions at small Reynolds numbers for the flow past a sphere and a circular cylinder. J. Fluid Mech. 2:237–262.

Robinson, J.A. (1995). Determination of flow patterns in a vertical crystalliser using computational fluid dynamics. BE thesis, James Cook University.

Shewchuk, J.R. (1996). Triangle: engineering a 2D quality mesh generator and Delaunay triangulator. In: Lin, M.C. and Manocha, D. (eds). Applied Computational Geometry, 203–222. Springer.

Sima, M.A. and Harris, J.A. (1997). Modelling of a low grade vertical cooling crystallizer using computational fluid dynamics. Proc. Aust. Soc. Sugar Cane Technol., 19:448–455.

Sima, M.A. and Harris, J.A. (1999). Numerical modelling of flow in a vertical cooling crystalliser. J. Fluids Engng, 121:148–154.

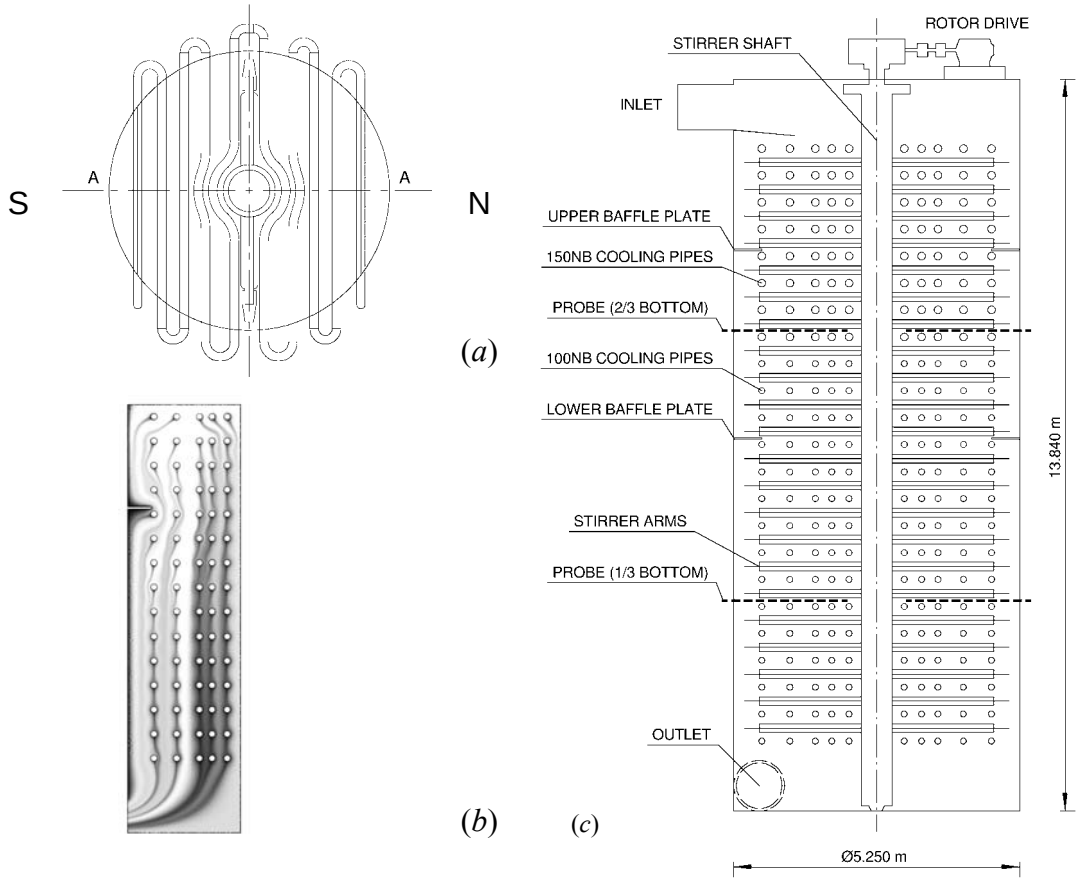

Fig. 1—Victoria Mill's vertical crystallizer: (*a*) plan; (*b*) *Triangle–Fastflo* temperature field in south half of A–A (black=cold, white=hot) while the vessel is two-thirds full, as was the case during the 2000 season traverses; (*c*) section A–A from east showing the four probe paths.

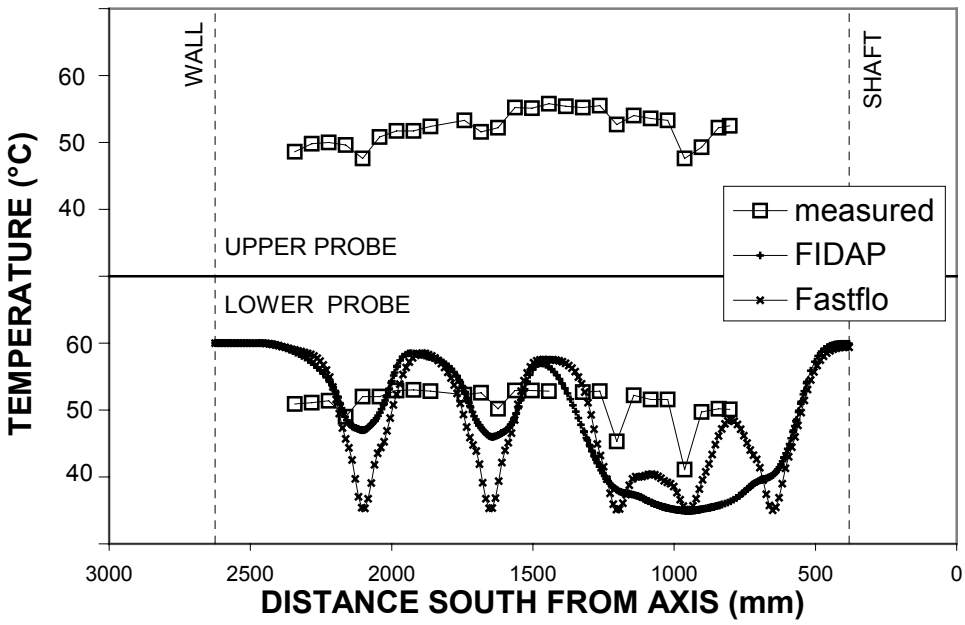

Fig. 2—Upper and lower south temperature profiles; including two CFD predictions at the lower level: temperature-thinning *FIDAP* and constant-viscosity *Triangle–Fastflo*.

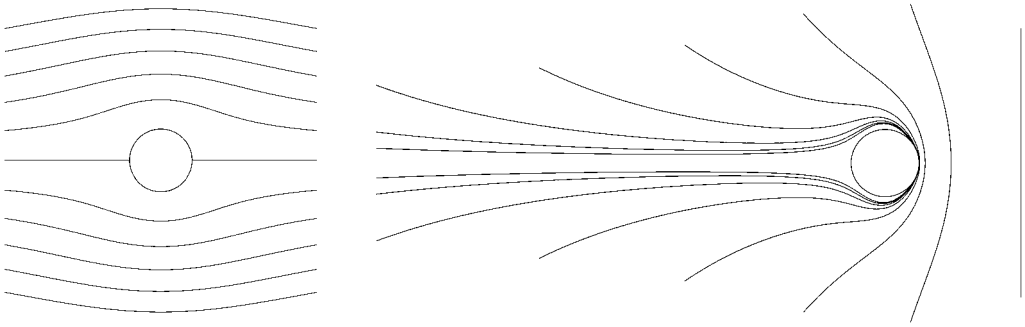

(*a*) (*b*)

Fig. 3—Relative motion of particles initially on a line perpendicular to and upstream (right) of a steadily moving cylinder, showing (*a*) streamlines, (*b*) material lines; obtained by integrating eq. 2.7 of Proudman and Pearson (1957) with *LSODE*, a Fortran subroutine for numerically integrating ordinary differential equations (Hindmarsh, 1983).

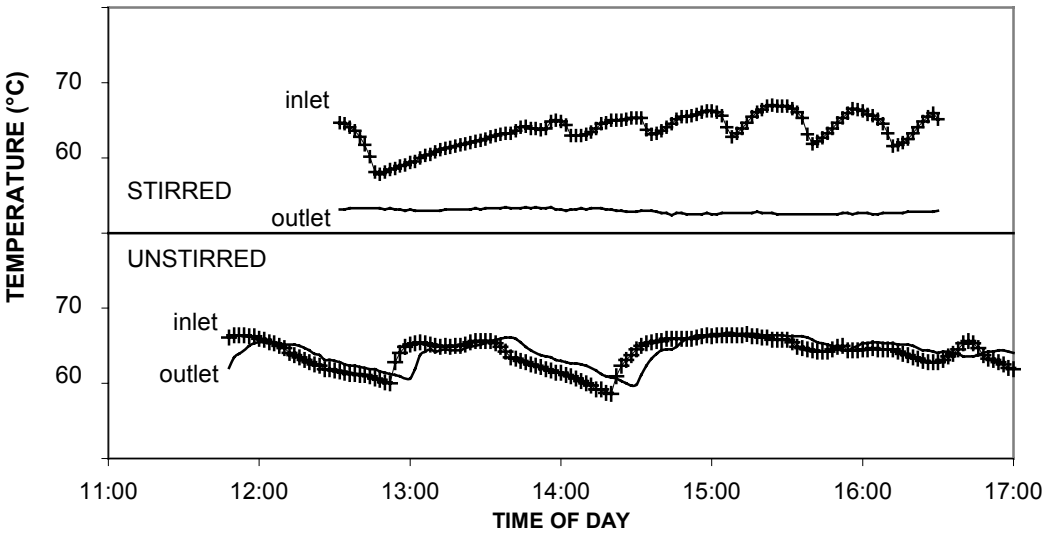

Fig. 4—Inlet and outlet massecuite temperatures during the stirring experiment.

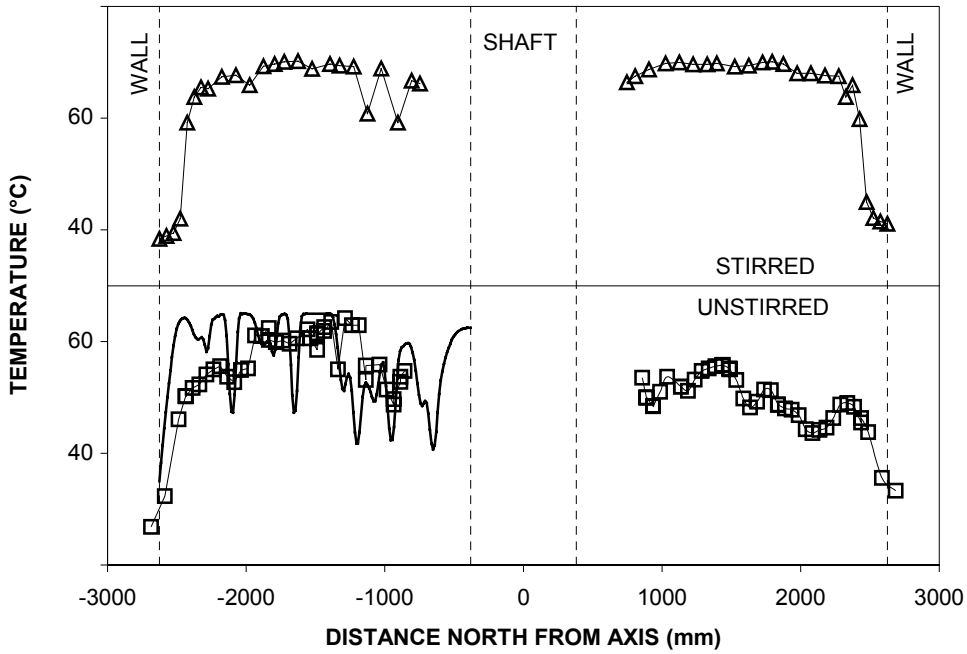

Fig. 5—Lower temperature profiles in the crystallizer with and without stirring. The curve without data points is from the *Triangle–Fastflo* solution in Figure 1*b*.